

Was the Progenitor of the Sagittarius Stream a Disc Galaxy?

Jorge Peñarrubia^{1*}, Vasily Belokurov¹, N.W. Evans¹, David Martínez-Delgado^{2,3}, Gerard Gilmore¹, Mike Irwin¹, Martin Niederste-Ostholt¹, Daniel B. Zucker^{4,5}

¹ *Institute of Astronomy, University of Cambridge, Madingley Road, Cambridge, CB3 0HA, UK*

² *Max Planck Institut für Astronomie, Königstuhl 17, 69117, Heidelberg, Germany*

³ *Instituto de Astrofísica de Canarias, La Laguna, Spain*

⁴ *Department of Physics, Macquarie University, North Ryde, NSW 2109, Australia*

⁵ *Anglo-Australian Observatory, PO Box 296, Epping, NSW 1710, Australia*

25 October 2018

ABSTRACT

We use N-body simulations to explore the possibility that the Sagittarius (Sgr) dwarf galaxy was originally a late-type, *rotating* disc galaxy, rather than a non-rotating, pressure-supported dwarf spheroidal galaxy, as previously thought. We find that bifurcations in the leading tail of the Sgr stream, similar to those detected by the SDSS survey, naturally arise in models where the Sgr disc is misaligned with respect to the orbital plane. Moreover, we show that the internal rotation of the progenitor may strongly alter the location of the leading tail projected on the sky, and thus affect the constraints on the shape of the Milky Way dark matter halo that may be derived from modelling the Sgr stream. Our models provide a clear, easily-tested prediction: although tidal mass stripping removes a large fraction of the original angular momentum in the progenitor dwarf galaxy, the remnant core should still rotate with a velocity amplitude $\sim 20 \text{ km s}^{-1}$ that could be readily detected in future, wide-field kinematic surveys of the Sgr dwarf.

Key words: galaxies: halos – Galaxy: evolution – Galaxy: formation – Galaxy: kinematics and dynamics

1 INTRODUCTION

In spite of extensive theoretical efforts undertaken to reproduce the characteristics of the Sagittarius (Sgr) stream (e.g. Ibata et al. 2001; Martínez-Delgado et al. 2004; Helmi 2004; Law et al. 2005, 2010; Fellhauer et al. 2006), there is presently no theoretical model that fully explains the wealth of available observational data. Two aspects of the stream have proved particularly challenging to model. First, the leading tail of the Sgr stream is bifurcated, with both arms exhibiting similar distances, velocities and metallicity distributions (Yanny et al. 2009; Niederste-Ostholt et al. 2010), which would appear to refute an earlier model explaining the bifurcation as two wraps of different ages (Fellhauer et al. 2006), or as independent streams from different progenitors. Second, the position on the sky of the stream suggests that the Milky Way (MW) dark matter halo interior to the stream has an oblate or perhaps a nearly spherical shape (Johnston et al. 2005; Fellhauer et al. 2006), while the heliocentric velocities of stream members support a prolate shape

(Helmi 2004). In a recent work, Law & Majewski (2010) (hereafter LM10) have shown that what appears as mutually exclusive results may in fact signal the possibility of the halo being triaxial in shape, as Cold Dark Matter (CDM) cosmological models predict (e.g. Kazantzidis et al. 2010 and references therein). However, LM10 find that in order to reproduce the location and velocities of the stream the intermediate axis of the dark matter halo should be aligned with the spin vector of the MW disc. This is hard to understand as circular orbits about the intermediate axis are unstable (e.g. Adams et al. 2007), raising questions as to the formation of the Galactic disc. Furthermore, this model does not attempt to explain the origin of the stream bifurcation.

Interestingly, the chemical composition of Sgr clearly stands out from the rest of MW dwarf spheroidal galaxies (dSphs). First, strong metallicity gradients ($-2.3 \lesssim [\text{Fe}/\text{H}] \lesssim 0.0$), unusual in other dwarfs, have been reported in the remnant core (Giuffrida et al. 2010), which also extends to the tidal tails (Chou et al. 2007; Monaco et al. 2007; Keller et al. 2010). Also, recent analysis of the chemical abundances in the core and tails of Sgr suggest that this galaxy underwent an enrichment history more akin to

* Email: jorpega,vasily,nwe@ast.cam.ac.uk

LMC than to other dSphs (Sbordone et al. 2007; Chou et al. 2010).

Motivated by the above results, here we explore the possibility that the Sgr dwarf was originally a late-type, rotating disc galaxy, rather than a pressure-supported dSph. The goal of this paper is to examine how rotation affects the properties of the associated tidal stream, and to provide model predictions that yield unambiguous tests for this scenario, rather than reproducing all of the well-documented properties of the Sgr stream in detail.

2 NUMERICAL MODELLING

The Galaxy model: The MW disc is assumed to follow a Miyamoto-Nagai (1975) model with a mass $M_d = 7.5 \times 10^{10} M_\odot$, and radial and vertical scale lengths $a = 3.5$ kpc and $b = 0.3$ kpc. The MW bulge follows a Hernquist (1990) profile with a mass $M_b = 1.3 \times 10^{10} M_\odot$ and a scale radius $c = 1.2$ kpc. The MW dark matter halo is modelled as a NFW profile with a virial mass $M_{\text{vir}} = 10^{12} M_\odot$, virial radius $r_{\text{vir}} = 258$ kpc and concentration $c_{\text{vir}} = 12$ (Klypin et al. 2002). Following LM10, we assume that the halo is triaxial in shape by introducing elliptical coordinates with the substitution $r \rightarrow m$, where $m^2 = x^2/a^2 + y^2/b^2 + z^2/c^2$, and (a, b, c) are dimensionless quantities. Following the results of LM10, we choose the density axis-ratios to be $(a, b, c) \simeq (0.61, 1.34, 1.22)$. The best-fitting models of LM10 also suggest that the Sun does not sit on one of the principal axes of the halo, but rather slightly off the x (i.e. minor)-axis, $(x_\odot, y_\odot) = R_\odot(-\cos[\lambda], \sin[\lambda])$, where $\lambda \simeq 10^\circ$. We hold the halo parameters fixed through the evolution of our Sgr models for simplicity given that tidal streams are barely sensitive to the past evolution of the host potential (Peñarrubia et al. 2006). Our analysis also neglects the effects of dynamical friction on the orbit of Sgr. However, dynamical friction is unlikely to introduce a strong orbital decay during the time-scale of interest (i.e. the last 2–3 Gyr, see Fig. 5 of Peñarrubia et al. 2006).

The orbit of Sgr: The current position of Sgr and its line-of-sight velocity in the Galactic standard of rest (GSR) frame are $(D, l, b) = (25\text{kpc}, 5^\circ.6, -14^\circ.2)$ and $v_{\text{los}} = 171$ km s⁻¹, respectively (Ibata et al. 1997). To derive the orbit of Sgr in the above potential, we adopt the proper motion estimates of Dinescu et al. (2005), who find $(\mu_l \cos b, \mu_b) = (-2.35 \pm 0.20, -2.07 \pm 0.20)$ mas/yr. Using the standard solar motion about the MW centre from Binney & Merrifield (1998), this translates into a space motion of $(u, v, w) \simeq (221, -74, 203)$ km s⁻¹. We use test particles to integrate its orbit back in time for a few orbital periods in order to provide initial conditions for our N-body realizations of the Sgr dwarf. We find that its orbital peri- and apocentres in the above potential are 15 and 67 kpc, respectively, which implies an orbital period of 1.04 Gyr. Currently, Sgr has just (≈ 34 Myr ago) gone through its last pericentric passage, and will cross the Milky Way disc in approximately 28 Myr.

N-body realizations of Sgr: We use the algorithm BUILDGAL to construct N-body realizations of late-type spirals composed of a baryonic disc and a dark matter halo (see Hernquist 1993 for a detailed description). The disc profile

is

$$\rho_d(R, z) = \frac{m_d}{4\pi R_d^2 z_0} \exp(-R/R_d) \text{sech}^2(z/z_0); \quad (1)$$

where m_d is the disc mass, z_0 is the vertical thickness, and R_d the radial scale-length. In our models we assume that $z_0 = 0.2R_d$. We adopt a non-singular isothermal profile for the dark matter halo

$$\rho_h(r) = \frac{m_h \alpha}{2\pi^{3/2} r_{\text{cut}}} \frac{\exp[-(r/r_{\text{cut}})^2]}{r^2 + r_c^2}, \quad (2)$$

where m_h is the halo mass, r_c is the core radius and $\alpha \simeq 1.156$. We find that the properties of the Sgr stream model are not particularly sensitive to the value of the core radius. Here we choose $r_c = 0.5R_d$.

We use the results of Nierderste-Ostholt et al. (2010) to crudely derive a fiducial mass for each of the components of our Sgr N-body models. These authors estimate that prior to stellar stripping Sgr had a total luminosity of $L \sim 10^8 L_\odot$, of which only 30–50% remains currently bound in the remnant core. In order to convert N-body masses into luminosities we adopt a constant stellar mass-to-light ratio of $\Upsilon_* = 3.5$ (note, however that the strong metallicity gradients measured throughout the Sgr core may indicate a large range of Υ_*). Under this choice the initial Sgr disc mass thus is $m_d \approx 3.5 \times 10^8 M_\odot$. Adopting a mass-to-light ratio of $\Upsilon = m_h/L \sim 24$, typical for dwarf galaxies with $L \sim 10^8 L_\odot$ (Mateo 1998), we have $m_h = 2.4 \times 10^9 M_\odot$. The total initial mass of our Sgr model therefore is $M = m_d + m_h = (\Upsilon_* + \Upsilon)L = 2.8 \times 10^9 M_\odot$. Also, since we only simulate the most recent history of the Sgr dwarf, our initial conditions must account for the fact that the outer halo envelope may have already been lost to tides at the time when the stellar stream begins to form (see Peñarrubia et al. 2008). To do this we impose a truncation in the dark matter density profile at $r = r_{\text{cut}} = 6R_d$, which roughly corresponds to the tidal radius of a satellite galaxy with mass $\sim 3 \times 10^9 M_\odot$ at a pericentre $r_{\text{peri}} = 15$ kpc.

The only remaining free parameter is the initial scale-length of our Sgr N-body models, R_d . We fix its value by demanding the bound remnants of the Sgr model to contain $\approx 50\%$ of its initial stellar mass at the final snap-shot of the simulation. Indeed, under this definition the value of R_d depends on the number of orbital periods for which we follow the evolution of the Sgr dwarf. Adopting an integration time of 2.5 orbital periods (see §3), this condition yields $R_d \simeq 0.9$ kpc. Under this choice of model parameters, the peak rotation velocity of Sgr is 43 km s⁻¹ at $R = 2.6R_d = 2.34$ kpc, which are indeed typical values for late-type spirals with luminosities $L \sim 10^8 L_\odot$ (e.g. Swaters et al. 2009).

The N-body code: We follow the evolution of the Sgr N-body model in the Galaxy potential using SUPERBOX, a highly efficient particle-mesh gravity code (see Fellhauer et al. 2000 for details). SUPERBOX uses three nested grid zones centered on the highest-density particle cell of the dwarf. Each grid has 128³ cubic cells: (i) the inner grid has a spacing of $dx = 3R_d/126 \simeq 2.4 \times 10^{-2} R_d$ and is meant to resolve the innermost region of the satellite galaxy. (ii) The middle grid extends to cover the whole dwarf, with spacing $10R_d/126$. (iii) The outermost grid extends out to $50 \times r_{\text{vir}}$ and is meant to follow particles that are stripped from the dwarf. We choose a constant time-step $\Delta t = 0.9$ Myr, which leads to a total energy conservation better than 1% after

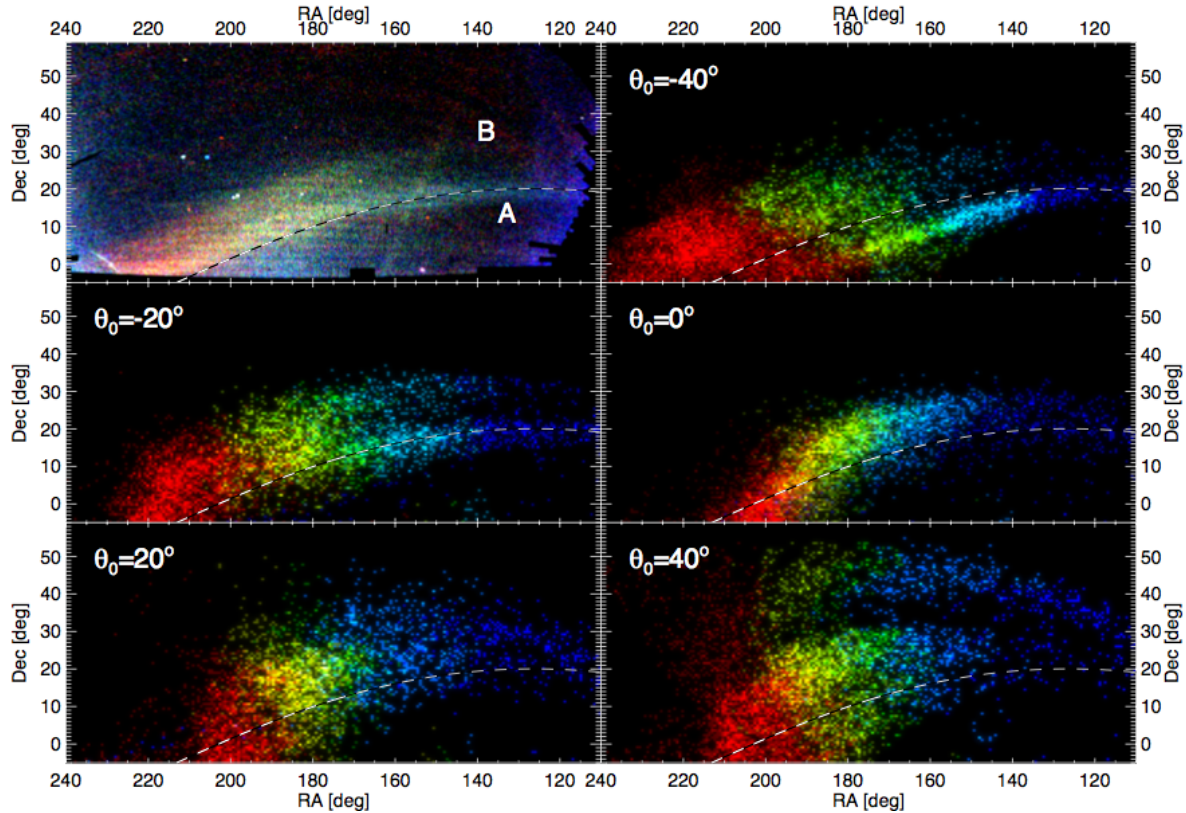


Figure 1. Leading tail particles in the “Field of Streams” area for different orientations of the Sgr disc with respect to its orbital plane (see text). SDSS data are shown in the upper-left panel. Our colour-coding denotes different heliocentric distances (blue, green and red for $D < 25$, 15–40 and 30–60 kpc, respectively). Dashed lines show a projection of the Sgr orbit integrated forward in time.

the dwarf models are evolved for a Hubble time in isolation. This shows that the evolution of the N-body model is free from artefacts induced by finite spatial and time resolutions.

3 RESULTS

The angle subtended by the internal angular momentum vector of Sgr and that of its orbit about the MW, i.e. $\theta_0 \equiv \text{acos}[\hat{\mathbf{J}}_{\text{int}} \cdot \hat{\mathbf{J}}_{\text{orb}}]$ is a free parameter in our study. The orientation of the Sgr disc is set at the start of the simulation by rotating \mathbf{J}_{int} an angle θ_0 about the instantaneous line of the orbit. Under this definition, $\theta_0 = 0$ denotes a model where the spin vector of the Sgr disc and the normal vector of the orbital plane are perfectly aligned, whilst $\theta_0 > 0$ and $\theta_0 < 0$ respectively indicate models where Sgr rotates in a prograde and retrograde motion with respect to its Galactic orbit.

Fig. 1 shows the projection on the “Field of streams” area of the sky (Belokurov et al. 2006) of Sgr stellar debris for different disc orientations after integrating our N-body models for 2.5 orbital periods. For simplicity, we show only particles that belong to the leading tail of the Sgr stream, given that the trailing tail has not been detected yet in the Northern Galactic Hemisphere. This Figure illustrates a few interesting points. The first is during the stripping process a fraction of the internal angular momentum of Sgr transfers to the stream. As a result, the stream tail(s) do not trace the progenitor’s orbit (dashed lines in Fig. 1). In practical

terms, our results suggest that internal rotation in the progenitor of the Sgr stream may have to be taken into account when inferring the shape of the MW halo from fitting the position and velocity of stream pieces. A second interesting point is that bifurcations in the leading tail of the Sgr stream naturally appear in this area of the sky if the spin vector and the normal vector of the orbital plane are misaligned. The separation between the bifurcated arms clearly becomes more prominent as the value of $|\theta_0|$ increases. Interestingly, by colour-coding the stellar particles according to their heliocentric distances, we can appreciate that in all models both arms show a very similar gradient throughout the sky, in concordance with observational data (Belokurov et al. 2006; Niederste-Ostholt et al. 2010). Hence, internal rotation in the Sgr dwarf mainly affects the apparent precession of the stream plane on the sky.

The model with $\theta_0 = -20^\circ$ has a striking resemblance with the Field of Streams. It also provides a reasonable match to most of the existing observational constraints. Fig. 2 shows the projected location (*upper panel*), heliocentric distance (*middle panel*) and line-of-sight velocity (*lower panel*) of the leading (open symbols) and trailing (closed symbols) tail particles of a Sgr stream model with initial orientation $\theta_0 = -20^\circ$. By colour-coding the particles according to the time at which they are stripped, we can appreciate that the bifurcation arises from material lost at consecutive pericentric passages. In particular, the southern, more prominent tail of the leading arm (stream A) corresponds to

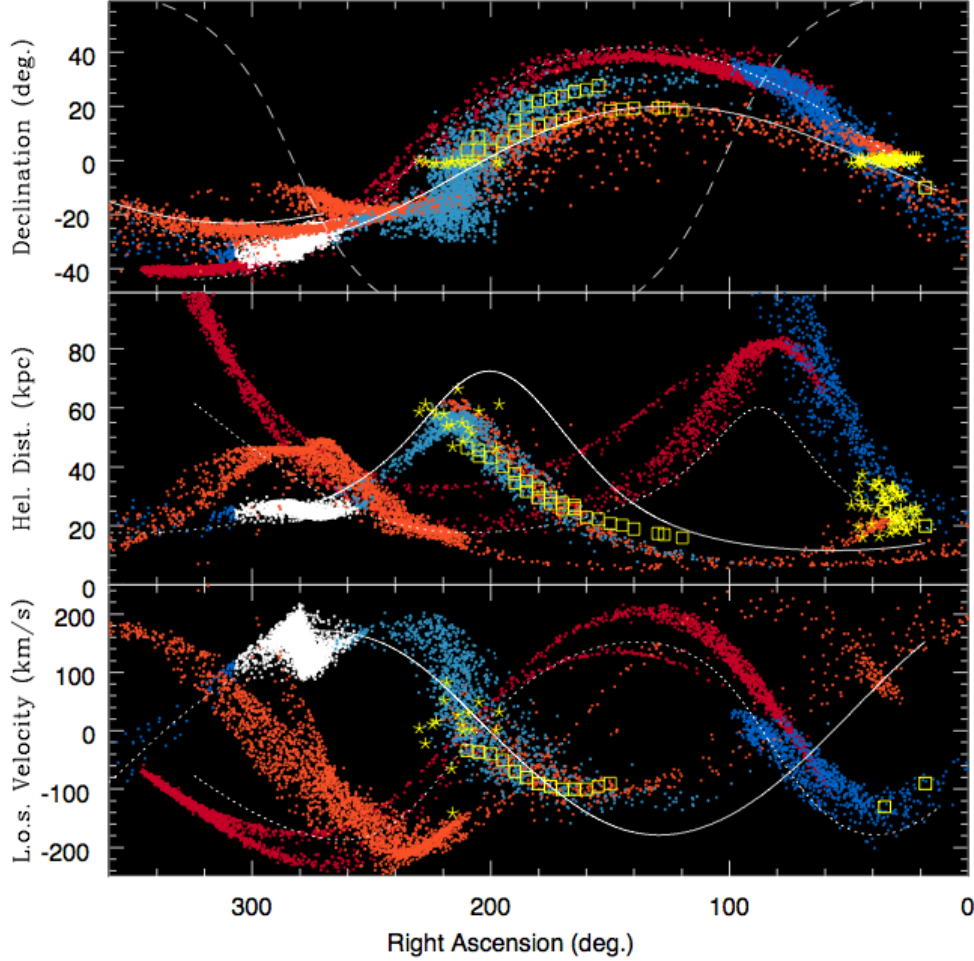


Figure 2. Projected location (*upper panel*), heliocentric distance (*middle panel*) and line-of-sight velocity (*lower panel*) in the GSR frame of the leading/trailing (light/dark colours) tail particles of a Sgr stream model with initial orientation $\theta_0 = -20^\circ$. Yellow stars and open squares denote RR Lyr (Vivas et al. 2005, Watkins et al. 2009) and SDSS detections of Sgr (Belokurov et al. 2006). White particles show the remnant core of the Sgr dwarf (see also Fig 3). The dashed line marks the position of the Galactic plane. For ease of reference we also show its orbit integrated forward (solid lines) and backward (dotted lines) in time. Note that the bifurcation of the leading arm arises from material stripped at different pericentric passages: blue at the penultimate pericentre passage ($\simeq 1$ Gyr ago) and red at the ante-penultimate one ($\simeq 2$ Gyr ago).

stars that were lost at the third most recent pericentric interaction, i.e. $\simeq 2$ Gyr ago (coloured in red), whilst the fainter northern tail (stream B) is more recent and is composed of stars that became unbound at the penultimate pericentre, i.e. $\simeq 1$ Gyr ago (in blue). This result clearly implies that the minimum age of the Sgr stream is two orbital periods, which justifies the choice of integration time for our N-body models.

This model correctly reproduces the distances and velocities measured along streams A and B, as well as the recent detections of the trailing tail in the southern hemisphere. Puzzlingly, although also predicted by our model, the presence of the trailing tail in the Field of Streams has thus far eluded detection. This may be explained by the drop of stars expected beyond the apocentre of the trailing tail, i.e. $\text{R.A.} \gtrsim 90^\circ$, as well as the sharp increase in distance at $\text{R.A.} \lesssim 120^\circ$, which may both conspire to put the surface brightness and the turn-off apparent magnitude of the

stream beyond the detection threshold of current photometric surveys.

Fig. 3 suggests that further clues on the nature of the Sgr dwarf may be gained by studying its remnant core. In the upper panel, we show the projection onto the sky of the Sgr dwarf model shown in Fig. 2. Particles are colour-coded according to the dwarf surface brightness at their location. The core morphology agrees well with that derived from the 2MASS survey (see e.g. Fig. 4 of Majewski et al. 2003), although its central surface brightness is somewhat brighter than estimated by these authors ($\mu_0 \simeq 24.8 \text{mag}/''^2$). Mismatches in surface brightness, however, may be a consequence of adopting a constant stellar mass-to-light ratio for our N-body particles. The lower panel of Fig. 3 shows that, although tidal mass stripping removes a large fraction of the original angular momentum in the progenitor Sgr disc, the remnant core is predicted to rotate with a velocity amplitude $\sim 20 \text{ km s}^{-1}$, which translates into a net velocity difference

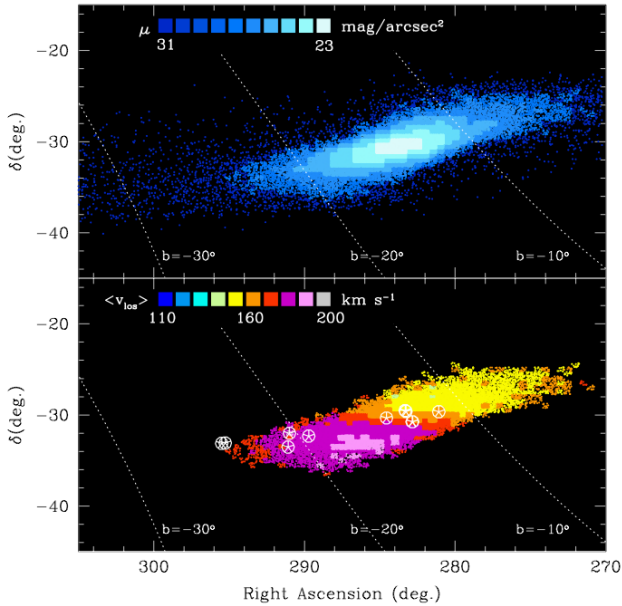


Figure 3. The remnant core of the Sgr dwarf model shown in Fig. 2. Particles are colour-coded according to the dwarf surface brightness at their location (*upper panel*) and mean line-of-sight velocity (*lower panel*). Symbols denote the location of the fields spectroscopically surveyed by Ibata et al. (1997). Note that our models predict that the remnant core still rotates with a velocity amplitude $\sim 20 \text{ km s}^{-1}$.

of $\sim 40 \text{ km s}^{-1}$ between stars at declinations above and below $\delta \sim -30^\circ$. Although not shown here, the central line of sight velocity dispersion is $\simeq 12 \text{ km s}^{-1}$, in reasonable agreement with the estimates of Bellazzini et al. (2008), who find a uniformly flat profile at $\sigma \simeq 10 \text{ km s}^{-1}$ over the central $0' \leq r \leq 9'$ range.

The only available kinematic survey throughout the Sgr dwarf dates back to Ibata et al. (1997). These authors measured a line-of-sight velocity between $160\text{--}170 \text{ km s}^{-1}$ in most of their pencil-beam fields, hence with little or no evidence of net rotation. Although in these locations our model accurately reproduces their velocity measurements, Fig. 3 suggests that Ibata et al. fields were too sparsely sampled to pick up the rotation signal predicted by our models.

4 CONCLUSIONS

Here, we explored the possibility that the Sgr was originally a late-type, rotating disc galaxy. We show that bifurcations in the leading tail of the Sgr stream, similar to those detected by the SDSS survey, naturally arise in models where the disc is misaligned with respect to the orbital plane. This occurs because material is primarily stripped at pericentric passages, and successive passages occur at different orientations of the Sgr disc. Together with observed metallicity patterns that are atypical for dwarf spheroidal galaxies, this suggests that the Sgr dwarf may have originally been a galaxy akin to late-type spirals with a peak rotation of $\gtrsim 45 \text{ km s}^{-1}$. We also find that internal rotation alters the position of the stream with respect the Sgr orbit, which might

indirectly affect any constraint on the shape of the MW halo derived from pressure-supported dwarf models.

Fortunately, before we embark upon more complex modelling of the Sgr stream, there is a clear-cut way to test whether the Sgr dwarf was indeed a rotating galaxy. Although tidal stripping efficiently removes angular momentum from the progenitor dwarf, we find that the remnant core should still rotate with a velocity amplitude close to $\sim 20 \text{ km s}^{-1}$ given the current estimates of the fraction of light residing in the tidal stream. Validating this prediction is feasible with existing instruments and will shed light on the true origin of the Sgr dwarf, as well as on the shape of the MW dark matter halo.

JP and MNO acknowledge financial support from the Science and Technology Facilities Council of the United Kingdom, whilst VB thanks for the Royal Society for financial support. This work has benefited greatly from discussions with D. Lynden-Bell. We thank the referee, D. Law, for his thorough read of this manuscript and his useful comments.

REFERENCES

- Adams, F. C., Bloch, A. M., Butler, S. C., Druce, J. M., & Ketchum, J. A. 2007, *ApJ*, 670, 1027
 Bellazzini, M., et al. 2008, *AJ*, 136, 1147
 Belokurov, V., et al. 2006, *ApJ*, 642, L137
 Binney, J., & Merrifield, M. 1998, *Galactic astronomy*, Princeton University Press, QB857 .B522 1998
 Chou, M.-Y., et al. 2007, *ApJ*, 670, 346
 Chou, M.-Y., Cunha, K., Majewski, S. R., Smith, V. V., Patterson, R. J., Martínez-Delgado, D., & Geisler, D. 2010, *ApJ*, 708, 1290
 Dinescu, D. I., Girard, T. M., van Altena, W. F., & López, C. E. 2005, *ApJ*, 618, L25
 Fellhauer, M., Kroupa, P., Baumgardt, H., Bien, R., Boily, C. M., Spurzem, R., & Wassmer, N. 2000, *New Astronomy*, 5, 305
 Fellhauer, M., et al. 2006, *ApJ*, 651, 167
 Giuffrida, G., Sbordone, L., Zaggia, S., Marconi, G., Bonifacio, P., Izzo, C., Szeifert, T., & Buonanno, R. 2010, *A&A*, 513, A62
 Helmi, A. 2004, *ApJ*, 610, L97
 Hernquist, L. 1990, *ApJ*, 356, 359
 Hernquist, L. 1993, *ApJS*, 86, 389
 Ibata, R. A., Gilmore, G., & Irwin, M. J. 1995, *MNRAS*, 277, 781
 Ibata, R., Lewis, G. F., Irwin, M., Totten, E., & Quinn, T. 2001, *ApJ*, 551, 294
 Johnston, K. V., Law, D. R., & Majewski, S. R. 2005, *ApJ*, 619, 800
 Kazantzidis, S., Abadi, M. G., & Navarro, J. F. 2010, arXiv:1006.0537
 Keller, S. C., Yong, D., & Da Costa, G. S. 2010, arXiv:1006.4885
 Klypin, A., Zhao, H., & Somerville, R. S. 2002, *ApJ*, 573, 597
 Law, D. R., Johnston, K. V., & Majewski, S. R. 2005, *ApJ*, 619, 807
 Law, D. R., & Majewski, S. R. 2010, *ApJ*, 714, 229 (LM10)

- Majewski, S. R., Skrutskie, M. F., Weinberg, M. D., & Ostheimer, J. C. 2003, *ApJ*, 599, 1082
- Martínez-Delgado, D., Gómez-Flechoso, M. Á., Aparicio, A., & Carrera, R. 2004, *ApJ*, 601, 242
- Mateo, M. L. 1998, *ARA&A*, 36, 435
- Miyamoto, M., & Nagai, R. 1975, *PASJ*, 27, 533
- Monaco, L., Bellazzini, M., Bonifacio, P., Buzzoni, A., Ferraro, F. R., Marconi, G., Sbordone, L., & Zaggia, S. 2007, *A&A*, 464, 201
- Niederste-Ostholt, M., Belokurov, V., Evans, N. W., & Peñarrubia, J. 2010, *ApJ*, 712, 516
- Peñarrubia, J., Benson, A. J., Martínez-Delgado, D., & Rix, H. W. 2006, *ApJ*, 645, 240
- Peñarrubia, J., Navarro, J. F., & McConnachie, A. W. 2008, *ApJ*, 673, 226
- Sbordone, L., Bonifacio, P., Buonanno, R., Marconi, G., Monaco, L., & Zaggia, S. 2007, *A&A*, 465, 815
- Swaters, R. A., Sancisi, R., van Albada, T. S., & van der Hulst, J. M. 2009, *A&A*, 493, 871
- Vivas, A. K., Zinn, R., & Gallart, C. 2005, *AJ*, 129, 189
- Watkins, L. L., et al. 2009, *MNRAS*, 398, 1757
- Yanny, B., et al. 2009, *ApJ*, 700, 1282